J. Math. Computer Sci., 36 (2025), 352–370

Online: ISSN 2008-949X

Journal of Mathematics and Computer Science

Journal Homepage: www.isr-publications.com/jmcs

Mathematical analysis of fractional order co-abuse infection model using power law type kernel

Izhar Ul Haq[a], Amjad Ali[a], Aman Ullah[b,*], Kamal Shah[b,c], Thabet Abdeljawad[c]

[a]*Department of Basic Sciences, University of Engineering and Technology, Khyber Pukhtunkhwa, Pakistan.*

[b]*Department of Mathematics, University of Malakand, Chakdara, Dir(L),18000, KPK, Pakistan.*

[c]*Department of Mathematics and Sciences, Prince Sultan University, Riyadh 11586, Saudi Arabia.*

Abstract

In this study, we present a mathematical model designed to illustrate the simultaneous occurrence of smoking and heroin co-abuse infections. To explore non-negative solutions and identify a stable equilibrium point, as well as the fundamental reproductive number, we enhance the model by integrating Caputo fractional-order (FO) derivative operators. Employing functional analysis concepts, we derive several results pertaining to the existence of a unique solution. Additionally, we utilize the Ulam-Hyres (UH) notion to establish the stability of the model solutions. To offer further insights, we present numerical results for the fractional-order system using an Euler-type numerical technique. These results are visually represented in graphs, illustrating the diverse responses of the model under different parameter values.

Keywords: Caputo operator, existence theoory, numerical techniques, unique solution.

2020 MSC: 26A33, 34A08, 35A09.

1. Introduction

Smoking typically involves the inhalation and exhalation of smoke produced by burning the leaves of the tobacco plant (Nicotiana tabacum). This practice is highly detrimental to the lungs due to the presence of over 4,000 chemicals in tobacco smoke that can cause significant damage. These chemicals include: (i) tar, which stains and harms lung tissue and is known to be carcinogenic, causing lung cancer; (ii) Nicotine, which can lead to the formation of sticky blood platelets and increase the risk of Cardiac heart illness; (iii) carbon monoxide, a toxic gas that impairs lung function and causes inflammation, increasing the likelihood of developing lung disease; (iv) Formaldehyde, another chemical present in tobacco smoke that can cause lung disease; (v) various metal ions such as arsenic, nickel, and cadmium, which are also known to be carcinogenic; (vi) radioactive compounds such as asbestos, which can contribute to the development of cancer.

*Corresponding author

Email addresses: izharulhaqbj095@gmail.com (Izhar Ul Haq), amjad.ali@uetpeshawar.edu.pk (Amjad Ali), amanswt@gmail.com (Aman Ullah), kamalshah408@gmail.com (Kamal Shah)

doi: 10.22436/jmcs.036.04.01

Received: 2023-12-21 *Revised:* 2023-12-28 *Accepted:* 2024-07-09

Smoking is a major global health issue and a leading cause of death, claiming the lives of over seven million people annually. Out of this number, six million are direct smokers, while approximately 900,000 are non-smokers who are exposed to secondhand smoke [36]. Middle-income countries are estimated to be home to around 80% of the world's 1.1 billion smokers, where they suffer from various smoking-related illnesses and fatalities. The economic impact of smoking is also significant, with an estimated global loss of two trillion dollars per year, equivalent to about 2% of the global economy. These losses are mainly due to decreased productivity caused by illness or death resulting from smoking and healthcare costs associated with treating smoking-related diseases, which account for approximately 30% of the economic burden.

Experts from various fields are conducting research on the link between smoking and heroin use. Governments around the world are actively proposing and implementing policies and laws aimed at addressing smoking and other forms of substance abuse. In [23], the authors presented findings that suggest that hospitals without a smoking policy may inadvertently cause patients to abruptly stop smoking upon admission. Abrupt cessation of drug use can affect drug metabolism, as cigarette smoking activates the Human Cytochromes P450 (CYP) 1A2 and 2B6. These enzymes are responsible for metabolizing many medically important drugs, such as clozapine, olanzapine, and methadone. After quitting smoking, decreased activity of CYP1A2 can lead to adverse drug reactions, including casing of chlozapine and olanzapine deadly. It is challenging to forecast the appropriate rebate in the dose of drugs metabolized by CYP 1A2 after smoking cessation. Therefore, therapeutic treatment should be closely monitored when possible. CYP1A2 activity remains unaffected by nicotine renewal therapy.

The creation of the initial mathematical framework of smoking conduct was attributed to Castillo et al. [8]. Since then, other articles have expanded on this model by adding new elements or creating new cohorts [11, 33]. In 2017, Matintu proposed a new adjustment that accounted for moderate, chain, occasional, and temporary smoking [24]. Some other mathematical investigations of smoking behaviour are given in the literature [7, 28, 32].

Heroin is an illegal drug derived from morphine, which is found in poppy seeds. The drug is typically inhaled or smoked, leading to respiratory and lung illnesses like pneumonia and tuberculosis. Heroin harms the respiratory system's mucosal tissue and reduces immunity. Throughout the latter half of the 20th century, several mathematical models emerged to elucidate the act of heroin abuse.

Wang and his collaborators developed the heroin epidemic model in 2011, using two bi-linear incidence laws instead of standard incidence laws. He claimed that the population fluctuates over time [34]. Samanta expanded the periodic epidemic model into a more sophisticated non-autonomous form through an extension [35]. Some nice works on heroin models are listed in [1, 9, 22].

Mathematical models are crucial in predicting the behaviour of infectious diseases and devising effective measures to inhibit their propagation in the future. To forecast transmission dynamics and reduce infection rates, researchers develop mathematical models. In the realm of epidemiology, there is a recent tendency to incorporate fractional-order (FO) derivative and integral operators into mathematical models. These operators offer greater flexibility compared to traditional deterministic models and have become a focal point in current mathematical research [12, 16, 17, 19]. Fractional-order (FO) differential equations feature fractional-order derivatives or integral operators that consider both past and current states. This characteristic makes them a potent tool for forecasting future states [4, 5, 18, 25]. They exhibit enhanced effectiveness when compared to classical deterministic operators, with Caputo and Riemann-Liouville operators being commonly employed in fractional-order differential equations [3, 13, 14, 26]. Differential equations find numerous applications in science and technology, including bifurcations, epidemiology and various other fields. The Caputo fractional operator is more effective tool for modeling complex dynamics and generating biologically plausible behavior. Compared to integer-order models, fractional-order (FO) models utilizing the Caputo operator produce more flexible outcomes. Furthermore, non-integer models accurately represent real-world phenomena by incorporating memory and heritable features [27, 30]. The FO models have been used in several fields of applied science such as biomathematics [6, 29, 39], engineering [15], mathematical physics [10, 31], and some other area [21, 37, 38].

In this paper, we apply the Caputo FO operator to transform Li et al. co-abuse model [20] into (FO) time derivative. We establish the existence and uniqueness of non-negative solutions for the model and demonstrate its different version of UH stability. We utilize an Euler-type numerical technique to get an estimated solution for the system. Finally, we conclude the paper with a summary of our findings. The structure of the paper is as follows. In Section 2, we introduce the description of the model. In Section 3, we introduce the fundamental concept of fractional calculus. Section 4, presents the primary findings of our research. Section 5 discusses numerical analysis of the model. Section 6, represents the numerical simulation. Finally, in Section 7, we provide the concluding remarks.

Assumptions

- People are consistently brought into the susceptible category through birth and immigration at a rate denoted by Λ.
- People become smokers by being influenced through their interactions with other individuals who smoke.
- Susceptible individuals adopt heroin use as a result of being influenced by their interactions with heroin users.
- Smokers transition to heroin use by engaging in interactive activities with heroin users in environments known for substance abuse, such as clubs, bars, etc.

2. Description of the co-abuse model

In this context, the overall population is denoted by $\mathbb{N}(t)$. This population is then divided into seven distinct sub-populations, which include:

- $\mathbb{S}(t)$ individuals who do not currently use cigarettes or heroin but are at risk of starting one of them;
- $\mathbb{U}_S$ individuals who use cigarettes but are not currently undergoing treatment;
- $\mathbb{U}_Q$ individuals who use heroin but are not currently undergoing treatment;
- $\mathbb{H}_S$ individuals who use cigarettes and are currently undergoing treatment;
- $\mathbb{G}_{SH}$ individuals who use both cigarettes and heroin but are not currently undergoing treatment;
- $\mathbb{R}_T$ individuals who use both cigarettes and heroin and are currently undergoing treatment;
- $\mathbb{R}$ individuals who recover from both cigarettes and heroin.

The model is as

$$\begin{cases} \frac{d\mathbb{S}}{dt} = \Lambda - \beta_1\Pi_1\mathbb{S} - \beta_2\Pi_2\mathbb{S} - \mu\mathbb{S}, \\ \frac{d\mathbb{U}_S}{dt} = \beta_1\Pi_1\mathbb{S} + \delta_2\mathbb{G}_{SH} + \xi_2\mathbb{R}_T + \rho_1\mathbb{U}_Q - \gamma_1\mathbb{U}_S - (\tau_1 + \rho_1 + \mu)\mathbb{U}_S, \\ \frac{d\mathbb{U}_Q}{dt} = \tau_1\mathbb{U}_S - (\rho_1 + \mu)\mathbb{U}_Q, \\ \frac{d\mathbb{H}_S}{dt} = \beta_2\Pi_2\mathbb{S} + \delta_1\mathbb{G}_{SH} + \xi_3\mathbb{R}_T + \rho_2\mathbb{R} - \gamma_2\Pi_2\mathbb{H}_S - (\tau_2 + \rho_2 + \mu)\mathbb{H}_S, \\ \frac{d\mathbb{G}_{SH}}{dt} = \gamma_1\Pi_1\mathbb{U} + \gamma_2\Pi_2\mathbb{H}_S + \xi_1\mathbb{R}_T - (\kappa_2 + \delta + \delta_1 + \delta_2 + \rho_3 + \mu)\mathbb{G}_{SH}, \\ \frac{d\mathbb{R}_T}{dt} = \tau_2\mathbb{H}_S + \delta\mathbb{G}_{SH} - (\kappa_3 + \xi + \xi_2 + \xi_3 + \mu)\mathbb{R}_T, \\ \frac{d\mathbb{R}}{dt} = \kappa_2\mathbb{G}_{SH} + \kappa_3\mathbb{R}_T - (\rho_2 + \mu)\mathbb{R}, \end{cases} \tag{2.1}$$

where initial values are provided as $\mathbb{S}(0) = \mathbb{S}^0$, $\mathbb{U}_S(0) = \mathbb{U}_S^0$, $\mathbb{U}_Q(0) = \mathbb{U}_Q^0$, $\mathbb{H}_S(0) = \mathbb{H}_S^0$, $\mathbb{G}_{SH}(0) = \mathbb{G}_{SH}^0$, $\mathbb{R}_T(0) = \mathbb{R}_T^0$, $\mathbb{R}(0) = \mathbb{R}^0$, where $\Pi_1 = \frac{\mathbb{U}_S + \varepsilon_1\mathbb{G}_{SH} + \varepsilon_2\mathbb{R}_T}{\mathbb{N}}$, $\Pi_2 = \frac{\mathbb{H}_S + \varepsilon_3\mathbb{G}_{SH} + \varepsilon_4\mathbb{R}_T}{\mathbb{N}}$.

The following is an explanation of the model's parameters. The parameter Λ corresponds to the rate at which individuals are recruited into the population. Π_1 is a parameter in the model that captures the exposure ratio of both smokers and heroin users those susceptible. τ_1 represents the ratio of individuals who are cigarette smokers but not under treatment. $\gamma_1\Pi_1$ is the rate at which individuals in the $\mathbb{U}_S$ class

begin to use heroin and move into the $\mathbb{G}_{SH}$ class. ξ_2 represents the ratio at which individuals in the $\mathbb{R}_T$ class return to the $\mathbb{U}_S$ class after successful heroin treatment. δ_2 represents the ratio at which individuals in the $\mathbb{R}_T$ class quit heroin use without treatment. ρ_1 is the ratio at which individuals who quit smoking in the $\mathbb{U}_S$ class start smoking again. Π_2 is the rate at which susceptible individuals enter the $\mathbb{H}_S$ class through contact with heroin users. $\gamma_2\Pi_2$ is the rate at which individuals in the $\mathbb{H}_S$ class move into the $\mathbb{G}_{SH}$ class through contact with smokers. ρ_1 represents the death ratio of individuals in the $\mathbb{U}_S$ class due to smoking. ρ_2 represents the death ratio of individuals in the $\mathbb{H}_S$ class due to heroin use. ρ_3 represents the death ratio of individuals in the $\mathbb{G}_{SH}$ class due to smoking and heroin use. δ_1 represents the ratio at which individuals in the co-abuse class $\mathbb{G}_{SH}$ quit smoking. ξ_3 represents the ratio at which individuals in the co-abuse class $\mathbb{G}_{SH}$ who only quit smoking during treatment may later relapse and become part of the heroin user group again. μ represents the death ratio of all individuals in the model. ϵ_i, where $i = 1, 2, 3, 4$, are modified parameters. The flow chart of our considered model is given in figure 1.

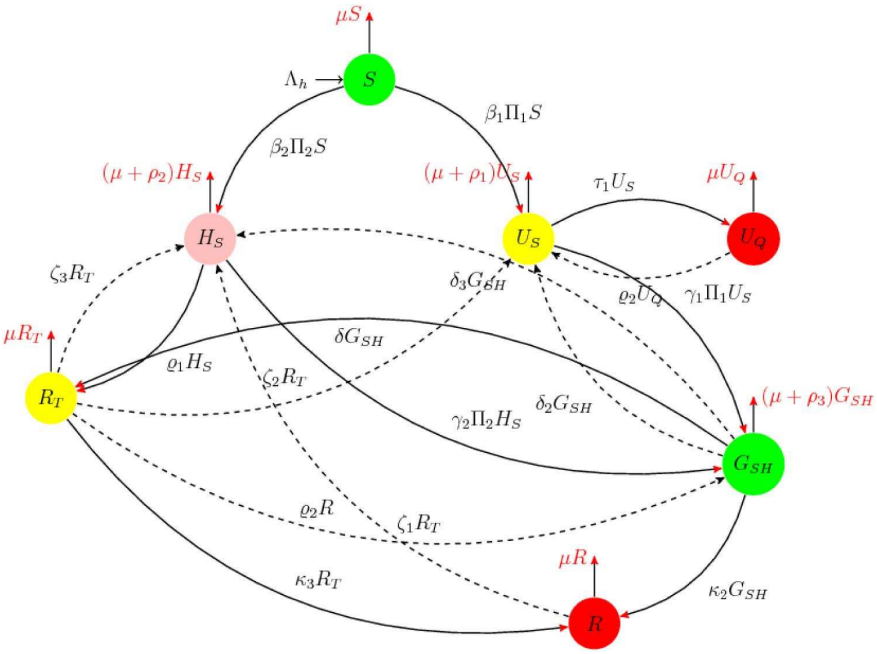

(a)

Figure 1: Diagram for all compartments.

3. Fractional order model

In this section, we presents a description of the suggest model (2.1) using Caputo FO operator. First we provide the definition of the Caputo operator.

Definition 3.1. Let $Z \in \mathbf{C}[0, T]$, then the Caputo operator is formally established as:

$$ {}^{C}\mathcal{D}_t^{\omega} Z(t) = \begin{cases} \frac{d^k z(t)}{dt^k}, & \omega = k \in N, \\ \frac{1}{\Gamma(k-\omega)} \int_0^t (t-x)^{k-\omega-1} Z^{(k)}(x)\,dx, & k-1 < \omega < k, k \in N. \end{cases} $$

Definition 3.2. Let $Z \in L^1([0, \mathbf{T}], \mathbb{R})$, Reimann-Liouville non-integers integral operator order $0 < \omega \leqslant 1$ is described as;

$$ \mathcal{I}_t^{\omega} Z(t) = \frac{1}{\Gamma(\omega)} \int_0^t (t-x)^{\omega-1} Z(x)\,dx. $$

Definition 3.3. If $\psi(s)$ is the Laplace transform of the function $\psi(t)$, then the Caputo fractional operator Laplace transform is given by:

$$\mathscr{L}\left[{}_{t_0}^{c}D_t^{\omega}\psi(t), s\right] = s^{\omega}\psi(s) - \sum_{i=0}^{n-1} s^{\omega-i-1}\psi^{(i)}(t_0), n-1 < \omega \leqslant n,$$

it is also written as

$$\mathscr{L}\left[{}_{t_0}^{c}D_t^{\omega}\psi(t), s\right] = \frac{s^{\omega}\psi(s) - s^{n-1}\psi(t_0) - s^{n-1}\psi^{1}(t_0) - \cdots - s^{n-1}\psi^{(n-1)}}{s^{n-\omega}}.$$

Caputo derivatives are defined using a singular-type kernel. Therefore, the proposed model (2.1) can be formulated using the singular Caputo model as follows in (3.1):

$$\begin{cases} {}^{C}\mathcal{D}_t^{\omega}\mathbb{S}(t) = \Lambda - \beta_1\Pi_1\mathbb{S} - \beta_2\Pi_2\mathbb{S} - \mu\mathbb{S}, \\ {}^{C}\mathcal{D}_t^{\omega}\mathbb{U}_S(t) = \beta_1\Pi_1\mathbb{S} + \delta_2\mathbb{G}_{SH} + \xi_2\mathbb{R}_T + \rho_1\mathbb{U}_Q - \gamma_1\mathbb{U}_S - (\tau_1+\rho_1+\mu)\mathbb{U}_S, \\ {}^{C}\mathcal{D}_t^{\omega}\mathbb{U}_Q(t) = \tau_1\mathbb{U}_S - (\rho_1+\mu)\mathbb{U}_Q, \\ {}^{C}\mathcal{D}_t^{\omega}\mathbb{H}_S(t) = \beta_2\Pi_2\mathbb{S} + \delta_1\mathbb{G}_{SH} + \xi_3\mathbb{R}_T + \rho_2\mathbb{R} - \gamma_2\Pi_2\mathbb{H}_S - (\tau_2+\rho_2+\mu)\mathbb{H}_S, \\ {}^{C}\mathcal{D}_t^{\omega}\mathbb{G}_{SH}(t) = \gamma_1\Pi_1\mathbb{U}_S + \gamma_2\Pi_2\mathbb{H}_S + \xi_1\mathbb{R}_T - (\kappa_2+\delta+\delta_1+\delta_2+\rho_3+\mu)\mathbb{G}_{SH}, \\ {}^{C}\mathcal{D}_t^{\omega}\mathbb{R}_T(t) = \tau_2\mathbb{H}_S + \delta\mathbb{G}_{SH} - (\kappa_3+\xi+\xi_2+\xi_3+\mu)\mathbb{R}_T, \\ {}^{C}\mathcal{D}_t^{\omega}\mathbb{R}(t) = \kappa_2\mathbb{G}_{SH} + \kappa_3\mathbb{R}_T - (\rho_2+\mu)\mathbb{R}, \end{cases} \tag{3.1}$$

where ${}^{C}\mathcal{D}_t^{\omega}$ is the caputo derivatives operator of fractional order ω.

4. Basic properties of the co-abuse Caputo model

4.1. Invariant region and attractively

The feasible region for the fractional co-abuse model (3.1) is denoted by Ψ and defined as a subset of the positive real numbers, i.e., $\Psi \subset \mathbb{R}_+^7$. This region represents the biologically feasible parameter values for the model,

$$\begin{aligned}\Psi = \{&\mathbb{S}(t), \mathbb{U}_S(t), \mathbb{U}_Q(t), \mathbb{H}_S(t), \mathbb{G}_{SH}(t), \mathbb{R}_T(t), \mathbb{R}(t) \epsilon \mathbb{R}_+^7 : \mathbb{S}(t) \\ &+ \mathbb{U}(t) + \mathbb{U}_Q(t) + \mathbb{H}_S(t) + \mathbb{G}_{SH}(t) + \mathbb{R}_T(t) + \mathbb{R}(t) \leqslant 1\}.\end{aligned}$$

Lemma 4.1. *The considered FO co-abuse model* (3.1) *with non-negative IVs in region* $\mathbb{R}_+^7$ *is positively invariant.*

Proof. Since

$$\begin{aligned}{}^{C}\mathcal{D}_t^{\omega}\mathbb{N}(t) =& {}^{C}\mathcal{D}_t^{\omega}\mathbb{S}(t) + {}^{C}\mathcal{D}_t^{\omega}\mathbb{U}_S(t) + {}^{C}\mathcal{D}_t^{\omega}\mathbb{U}_Q(t) \\ &+ {}^{C}\mathcal{D}_t^{\omega}\mathbb{H}_S(t) + {}^{C}\mathcal{D}_t^{\omega}\mathbb{G}_{SH}(t) + {}^{C}\mathcal{D}_t^{\omega}\mathbb{R}_T(t) + {}^{C}\mathcal{D}_t^{\omega}\mathbb{R}(t) \\ &= \Lambda - \mu\mathbb{N} - \rho_1\mathbb{U}_S - \rho_2\mathbb{H}_S - \rho_3\mathbb{G}_{SH} \leqslant \Lambda - \mu\mathbb{N} {}^{C}\mathcal{D}_t^{\omega}\mathbb{N}(t) + \mu\mathbb{N}(t) \leqslant \Lambda.\end{aligned}$$

By applying LT, we reach

$$L\left[{}^{C}\mathcal{D}_t^{\omega}\mathbb{N}(t) + \mu\mathbb{N}(t)\right] \leqslant L[\Lambda], \quad s^{\omega}\mathbb{N}(s) - s^{\omega-1}\mathbb{N}(0) + \mu\mathbb{N}(s) \leqslant \frac{\Lambda}{s}, \quad \mathbb{N}(s)\left[s^{\omega}+\mu\right] \leqslant s^{\omega-1}\mathbb{N}(0) + \frac{\Lambda}{s}.$$

Via inverse LT, one gets

$$L^{-1}[\mathbb{N}(s)] \leqslant L^{-1}\left[\frac{s^{\omega-1}\mathbb{N}(0)}{s^{\omega}+\mu} + \frac{\Lambda}{s(s^{\omega}+\mu)}\right], \qquad \mathbb{N}(s) \leqslant \mathbb{N}(0)E_{\omega,1}(-\mu t^{\omega}) + \Lambda t^{\omega}E_{\omega,\omega+1}(-\mu t^{\omega}).$$

Consequently, as $t \to \infty$, $\mathbb{N}(t)$ converges, and thus the region Ψ is positively invariant in $\mathbb{R}_+^7$. Further, for $t \to \infty$, the total population is bounded by $\frac{\Lambda}{\mu}$. □

4.2. Equilibrium points (EPs)

4.2.1. DFEPs

The EP that is free from co-abuse, represented as E^0, is present in a community where there are no individuals who smoke or use heroin. Thus, from [20], one has

$$E^0 = (\mathbb{S}^0, \mathbb{U}_S^o, \mathbb{U}_Q^0, \mathbb{H}_S^0, \mathbb{G}_{SH}^0, \mathbb{R}_T^0, \mathbb{R}^0) = \left(\frac{\Lambda}{\mu}, 0, 0, 0, 0, 0, 0\right).$$

4.2.2. DEEPs

The EP that is affected by co-abuse, denoted as non-E^*, exists in a community where there are individuals who smoke or use heroin. To calculate the endemic EP of model (2.1) in relation to the infection forces ($\prod_1$, $\prod_2$), we use the following formula:

$$E^* = \begin{cases} \mathbb{S}^* = \frac{\Lambda}{\beta_1\Pi_1+\beta_2\Pi_2+\mu}, \\ \mathbb{U}_S^* = \frac{\beta_2 D_1\Pi_2 S+(\xi_2\delta_2 D_1+\delta)\mathbb{G}_{SH}+\xi_2\tau_2\mathbb{H}_S}{D_1(\rho_1(\rho_1+\mu)+\mu(\tau_1+\rho_1+\mu))}, \\ \mathbb{U}_Q^* = \frac{\tau_1\mathbb{U}_S}{\rho_1+\mu}, \\ \mathbb{H}_S^* = \frac{\beta_2\Pi_2(\rho_2+\mu)D_1 S}{(\gamma_2\Pi_2+\rho_2+\mu)(\rho_2+\mu)D_1+\tau_2(\xi_1+\xi_2+\mu)+\tau_2\mu\kappa_3} + \frac{(D_1(\delta_1(\rho_2+\mu)+\rho_2\kappa_3)+\xi_3(\rho_2+\mu)(\delta+\tau_2)+\rho_2\kappa_3\delta)\mathbb{G}_{SH}}{(\gamma_2\Pi_2+\rho_2+\mu)(\rho_2+\mu)D_1+\tau_2(\xi_1+\xi_2+\mu)+\tau_2\mu\kappa_3}, \\ \mathbb{G}_{SH}^* = \frac{\gamma_1 D_1\Pi_1\mathbb{U}_S+(\gamma_2\Pi_2+\xi_2\tau_2)\mathbb{H}_S}{\delta(\kappa_3+\xi_2+\xi_3+\mu)+(\kappa_2+\delta_1+\delta_2+\rho_3+\mu)D_1}, \\ \mathbb{R}_T^* = \frac{\delta\mathbb{G}_{SH}+\tau_2\mathbb{H}_S}{D_1}, \\ \mathbb{R}^* = \frac{(\kappa_2 D_1+\kappa_3\delta)\mathbb{G}_{SH}+\tau_2\kappa_3\mathbb{H}_S}{(\rho_2+\mu)D_1}. \end{cases}$$

4.3. Reproduction number (RN)

Following the techniques of [20], we can obtain the basic RN. Let $X = (\mathbb{U}_S, \mathbb{H}_S, \mathbb{G}_{SH}, \mathbb{R}_T)$, and rewrite the model (2.1) as $\frac{dX}{dt} = F - V$, where

$$F = \begin{bmatrix} \beta_1\Pi_1\mathbb{S}+\gamma_1\Pi_1\mathbb{U}_S \\ \beta_2\Pi_2\mathbb{S}+\gamma_2\Pi_2\mathbb{H}_S \\ \gamma_1\Pi_1\mathbb{U}_S+\gamma_2\Pi_2\mathbb{H}_S \\ 0 \end{bmatrix}.$$

The following expression can be obtained by computing the partial derivative of F with respect to the free EP:

$$\mathcal{F} = \begin{bmatrix} \frac{\beta_1 S}{N} & 0 & \frac{\beta_1\varepsilon_1 S}{N} & \frac{\beta_1\varepsilon_2 S}{N} \\ 0 & \frac{\beta_2 S}{N} & \frac{\beta_2\varepsilon_3 S}{N} & \frac{\beta_2\varepsilon_4 S}{N} \\ 0 & 0 & 0 & 0 \\ 0 & 0 & 0 & 0 \end{bmatrix}.$$

Next,

$$V = \begin{bmatrix} (\tau_1+\rho_1+\mu)\mathbb{U}_S-\delta_2\mathbb{G}_{SH}-\xi_2\mathbb{R}_T-\rho_1\mathbb{U}_Q \\ (\tau_2+\rho_2+\mu)\mathbb{H}_S-\delta_1\mathbb{G}_{SH}-\xi_3\mathbb{R}_T-\rho_2\mathbb{R} \\ (\kappa_2+\delta+\delta_1+\delta_2+\rho_3+\mu)\mathbb{G}_{SH}-\xi_1\mathbb{R}_T \\ (\kappa_3+\xi+\xi_2+\xi_3+\mu)\mathbb{R}_T-\tau_2\mathbb{H}_S-\delta\mathbb{G}_{SH}. \end{bmatrix}.$$

Also,

$$\mathcal{V}^{-1} = \begin{bmatrix} (\tau_1+\rho_1+\mu) & 0 & -\delta_2 & -\xi_2 \\ 0 & (\tau_2+\rho_2+\mu) & -\delta_1 & -\xi_3 \\ 0 & 0 & (\kappa_2+\delta+\delta_1+\delta_2+\rho_3+\mu) & \xi_1 \\ 0 & -\tau_2 & -\delta & (\kappa_3+\xi_1+\xi_2+\xi_3+\mu). \end{bmatrix}.$$

Hence, the next matrix for the model is as

$$F\mathcal{V}^{-1} = \begin{bmatrix} \frac{\beta_1 S}{N(\tau_1+\rho_1+\mu)} & b_{12} & b_{13} & b_{14} \\ 0 & b_{22} & b_{23} & b_{24} \\ 0 & 0 & 0 & 0 \\ 0 & 0 & 0 & 0 \end{bmatrix},$$

and $b_{12}, b_{13}, b_{14}, b_{22}, b_{23}$, and b_{24} are given in [20]. Next, we have $D_0 = (\delta + \kappa_2 + \delta_1 + \delta_2 + \rho_3 + \mu)$, $D_1 = (\mu + \kappa_3 + \xi_1 + \xi_2 + \xi_3)$, $F_0 = \frac{\xi_2(\delta(\rho_2+\mu)+(\delta+\delta_1)\tau_2)+\delta_2(-\xi_2\tau_2+D_1(\rho_2+\tau_2+\mu))}{\rho_1+\tau_1+\mu}$. The spectral radius $R_{HS}$of the matrix $F\mathcal{V}^{-1}$, is the basic RN. The RN $R_{HS} = \max\{R_{0,1}, R_{0,2}\}$, here

$$R_{0,1} = \frac{S\beta_1}{N(\rho_1+\tau_1+\mu)}, \qquad R_{0,2} = \frac{S\beta_2(-\delta\xi + D_0D_1 + \varepsilon_3\xi_1\tau_2 + \varepsilon_4D_0\tau_2}{N(-\xi_1(\delta(\rho_2+\mu)+(\delta+\delta_1)\tau_2)+D_0(-\xi_3\tau_2+D_0(\rho_2+\tau_2+\mu))}.$$

4.4. Existence and uniqueness

Here, we deduce some theorems related to existence of unique solution of the considered co-abuse FO system (3.1). We begin by defining a norm as follows:

$$\left\|(S, U_S, U_Q, H_S, G_{SH}, R_T, R)\right\| = \|S\| + \|U_S\| + \left\|U_Q\right\| + \|H\| + \|G_{SH}\| + \|R_T\| + \|R\|,$$

where $\|S\| = \sup\{|S(t)| : t\epsilon I\}$, $\|U_S\| = \sup\{|U_S(t)| : t\epsilon I\}$, $\left\|U_Q\right\| = \sup\{\left|U_Q(t)\right| : t\epsilon I\}$, $\|H_S\| = \sup\{|H_S(t)| : t\epsilon I\}$, $\|G_{SH}\| = \sup\{|G_{SH}(t)| : t\epsilon I\}$, $\|R_T\| = \sup\{|R_T(t)| : t\epsilon I\}$, $\|R\| = \sup\{|R(t)| : t\epsilon I\}$, and $B = \sigma(I) \times \sigma(I) \times \sigma(I) \times \sigma(I) \times \sigma(I) \times \sigma(I) \times \sigma(I)$, defined the Banach space real valued continuous mapping on the interval I and related supremum norm. For convenience, we can express the model (3.1) in an equivalent form, which is specified in (4.1):

$$\begin{cases} {}^{C}\mathcal{D}_t^{\omega} S(t) = G_1(t, S), \\ {}^{C}\mathcal{D}_t^{\omega} U_S(t) = G_2(t, U_S), \\ {}^{C}\mathcal{D}_t^{\omega} U_Q(t) = G_3(t, U_Q), \\ {}^{C}\mathcal{D}_t^{\omega} H_S(t) = G_4(t, H_S), \\ {}^{C}\mathcal{D}_t^{\omega} G_{SH}(t) = G_5(t, G_{SH}), \\ {}^{C}\mathcal{D}_t^{\omega} R_T(t) = G_6(t, R_T), \\ {}^{C}\mathcal{D}_t^{\omega} R(t) = G_7(t, R). \end{cases} \tag{4.1}$$

Equivalently, we have from (4.1), the following system (4.2)

$$\begin{cases} S(t) - S(0) = \frac{1}{\Gamma(\omega)} \int_0^t (t-x)^{\omega-1} G_1(x, S)dx, \\ U_S(t) - U_S(0) = \frac{1}{\Gamma(\omega)} \int_0^t (t-x)^{\omega-1} G_2(x, U_S)dx, \\ U_Q(t) - U_Q(0) = \frac{1}{\Gamma(\omega)} \int_0^t (t-x)^{\omega-1} G_3(x, U_Q)dx, \\ H_S(t) - H_S(0) = \frac{1}{\Gamma(\omega)} \int_0^t (t-x)^{\omega-1} G_4(x, H_S)dx, \\ G_{SH}(t) - G_{SH}(0) = \frac{1}{\Gamma(\omega)} \int_0^t (t-x)^{\omega-1} G_5(x, G_{SH})dx, \\ R_T(t) - R_T(0) = \frac{1}{\Gamma(\omega)} \int_0^t (t-x)^{\omega-1} G_6(x, R_T)dx, \\ R(t) - R(0) = \frac{1}{\Gamma(\omega)} \int_0^t (t-x)^{\omega-1} G_7(x, R)dx. \end{cases} \tag{4.2}$$

Let

$$Q(t) = \begin{pmatrix} S(t) \\ U_S(t) \\ U_Q(t) \\ H_S(t) \\ G_{SH}(t) \\ R_T(t) \\ R(t) \end{pmatrix}, \qquad W(t, Q(t)) = \begin{pmatrix} G_1(t, X_1) \\ G_2(t, I_1) \\ G_3(t, Z_1) \\ G_4(t, X_1) \\ G_5(t, X_1) \\ G_6(t, X_1) \\ G_7(t, X_1) \end{pmatrix}, \qquad Q(0) = \begin{pmatrix} S(0) \\ U_S(0) \\ U_Q(0) \\ H_S(0) \\ G_{SH}(0) \\ R_T(0) \\ R(0) \end{pmatrix}.$$

From (4.2) we get (4.3)

$$\mathbb{Q}(t) = \mathbb{Q}_0 - \frac{1}{\Gamma(\omega)} \int_0^t (t-x)^{\omega-1} \mathbb{W}(x, \mathbb{Q}(x)) dx. \tag{4.3}$$

Now we check that the kernels $G_1, G_2, \ldots, G_7$ are agree with the Lipschiz constraint and contraction under some retention. We have analyzed for G_1, in the next theorem and same can be proved for the rest of equations.

Theorem 4.2. *Let* $0 < \{\beta_1\Pi_1 + \beta_2\Pi_2 + \mu\} < 1$. *The kernel* G_1, *agrees the Lipschiz property as well as contraction.*

Proof. For $\mathbb{S}$ and $\mathbb{S}_1$,

$$\begin{aligned} \|G_1(t,\mathbb{S}) - G_1(t,\mathbb{S}_1)\| &= \|\Lambda - \beta_1\Pi_1\mathbb{S} - \beta_2\Pi_2\mathbb{S} - \mu\mathbb{S} - \Lambda + \beta_1\Pi_1\mathbb{S} + \beta_2\Pi_2\mathbb{S} + \mu\mathbb{S}\| \\ &= \|\beta_1\Pi_1(\mathbb{S}-\mathbb{S}_1) + \beta_2\Pi_2(\mathbb{S}-\mathbb{S}_1) + \mu(\mathbb{S}-\mathbb{S}_1)\| \\ &\leqslant \beta_1\Pi_1 \|(\mathbb{S}-\mathbb{S}_1)\| + \beta_2\Pi_2 \|(\mathbb{S}-\mathbb{S}_1)\| + \mu \|(\mathbb{S}-\mathbb{S}_1)\|. \end{aligned}$$

We can write the above relation as

$$\|G_1(t,\mathbb{S}) - G_1(t,\mathbb{S}_1)\| \leqslant (\beta_1\Pi_1 + \beta_2\Pi_2 + \mu) \|\mathbb{S}(t) - \mathbb{S}_1(t)\|, \quad \|G_1(t,\mathbb{S}) - G_1(t,\mathbb{S}_1)\| \leqslant \mathfrak{L}_1 \|\mathbb{S}(t) - \mathbb{S}_1(t)\|,$$

where $\mathfrak{L}_1 = [\beta_1\Pi_1 + \beta_2\Pi_2 + \mu]$ implies that

$$\|G_1(t,\mathbb{S}) - G_1(t,\mathbb{S}_1)\| \leqslant \mathfrak{L}_1 \|\mathbb{S}(t) - \mathbb{S}_1(t)\|.$$

Under the Lipschiz condition with constant $0 < \{\beta_1\Pi_1 + \beta_2\Pi_2 + \mu\} < 1$, we get that G_1 is a contraction as shown bellow:

$$\|G_1(t,\mathbb{S}) - G_1(t,\mathbb{S}_1)\| \leqslant \mathfrak{L}_1 \|\mathbb{S}(t) - \mathbb{S}_1(t)\|.$$

□

For the remaining classes, one may prove the following:

$$\|G_2(t,\mathbb{U}_S) - G_2(t,\mathbb{U}_{S1})\| \leqslant \mathfrak{L}_2 \|\mathbb{U}_S(t) - \mathbb{U}_{S1}(t)\|, \quad \left\|G_3(t,\mathbb{U}_Q) - G_3(t,\mathbb{U}_{Q1})\right\| \leqslant \mathfrak{L}_3 \left\|\mathbb{U}_Q(t) - \mathbb{U}_{Q1}(t)\right\|,$$
$$\|G_4(t,\mathbb{H}_S) - G_4(t,\mathbb{H}_{S1})\| \leqslant \mathfrak{L}_4 \|\mathbb{H}_S(t) - \mathbb{H}_{S1}(t)\|, \quad \|G_5(t,\mathbb{G}_{SH}) - G_5(t,\mathbb{G}_{SH})\| \leqslant \mathfrak{L}_5 \|\mathbb{G}_{SH}(t) - \mathbb{G}_{SH1}(t)\|,$$
$$\|G_6(t,\mathbb{R}_T) - G_6(t,\mathbb{R}_{T1})\| \leqslant \mathfrak{L}_6 \|\mathbb{R}_T(t) - \mathbb{R}_{T1}(t)\|, \qquad \|G_7(t,\mathbb{R}) - G_7(t,\mathbb{R}_1)\| \leqslant \mathfrak{L}_7 \|\mathbb{R}(t) - \mathbb{R}_1(t)\|.$$

Recursively, (4.2) can be given as

$$\mathbb{S}_n(t) - \mathbb{S}(0) = \frac{1}{\Gamma(\omega)} \int_0^t (t-x)^{\omega-1} G_1(x, \mathbb{S}_{n-1}) dx, \qquad \mathbb{U}_{Sn}(t) - \mathbb{U}_S(0) = \frac{1}{\Gamma(\omega)} \int_0^t (t-x)^{\omega-1} G_2(x, \mathbb{U}_{Sn-1}) dx,$$
$$\mathbb{U}_{Qn}(t) - \mathbb{U}_Q(0) = \frac{1}{\Gamma(\omega)} \int_0^t (t-x)^{\omega-1} G_3(x, \mathbb{U}_{Qn-1}) dx, \quad \mathbb{H}_{Sn}(t) - \mathbb{H}_S(0) = \frac{1}{\Gamma(\omega)} \int_0^t (t-x)^{\omega-1} G_4(x, \mathbb{H}_{Sn-1}) dx,$$
$$\mathbb{G}_{SHn}(t) - \mathbb{G}_{SH}(0) = \frac{1}{\Gamma(\omega)} \int_0^t (t-x)^{\omega-1} G_5(x, \mathbb{G}_{SHn-1}) dx, \quad \mathbb{R}_{Tn}(t) - \mathbb{R}_T(0) = \frac{1}{\Gamma(\omega)} \int_0^t (t-x)^{\omega-1} G_6(x, \mathbb{R}_{Tn-1}) dx,$$
$$\mathbb{R}_n(t) - \mathbb{R}(0) = \frac{1}{\Gamma(\omega)} \int_0^t (t-x)^{\omega-1} G_7(x, \mathbb{R}_{n-1}) dx.$$

Now, consider

$$\Phi_{1n}(t) = \mathbb{S}_n(t) - \mathbb{S}_{n-1}(t) = \frac{1}{\Gamma(\omega)} \int_0^t (t-x)^{\omega-1} (G_1(x, \mathbb{S}_{n-1}) - G_1(x, \mathbb{S}_{n-2})) dx,$$

$$\Phi_{2n}(t) = \mathbb{U}_{Sn}(t) - \mathbb{U}_{Sn-1}(t) = \frac{1}{\Gamma(\omega)}\int_0^t (t-x)^{\omega-1}(G_2(x,\mathbb{U}_{Sn-1}) - G_2(x,\mathbb{U}_{Sn-2}))dx,$$

$$\Phi_{3n}(t) = \mathbb{U}_{Qn}(t) - \mathbb{U}_{Qn-1}(t) = \frac{1}{\Gamma(\omega)}\int_0^t (t-x)^{\omega-1}(G_3(x,\mathbb{U}_{Qn-1}) - G_3(x,\mathbb{U}_{Qn-2}))dx,$$

$$\Phi_{4n}(t) = \mathbb{H}_{Sn}(t) - \mathbb{H}_{Sn-1}(t) = \frac{1}{\Gamma(\omega)}\int_0^t (t-x)^{\omega-1}(G_4(x,\mathbb{H}_{Sn-1}) - G_4(x,\mathbb{H}_{Sn-2}))dx,$$

$$\Phi_{5n}(t) = \mathbb{G}_{SHn}(t) - \mathbb{G}_{SHn-1}(t) = \frac{1}{\Gamma(\omega)}\int_0^t (t-x)^{\omega-1}(G_5(x,\mathbb{G}_{SHn-1}) - G_5(x,\mathbb{G}_{SHn-2}))dx,$$

$$\Phi_{6n}(t) = \mathbb{R}_{Tn}(t) - \mathbb{R}_{Tn-1}(t) = \frac{1}{\Gamma(\omega)}\int_0^t (t-x)^{\omega-1}(G_6(x,\mathbb{R}_{Tn-1}) - G_6(x,\mathbb{R}_{Tn-2}))dx,$$

$$\Phi_{7n}(t) = \mathbb{R}_{n}(t) - \mathbb{R}_{n-1}(t) = \frac{1}{\Gamma(\omega)}\int_0^t (t-x)^{\omega-1}(G_7(x,\mathbb{R}_{n-1}) - G_7(x,\mathbb{R}_{n-2}))dx,$$

with IVs $\mathbb{S}_0(t) = \mathbb{S}(0)$, $\mathbb{U}_{S0}(t) = \mathbb{U}_S(0)$, $\mathbb{U}_{Q0}(t) = \mathbb{U}_Q(0)$, $\mathbb{H}_{S0}(t) = \mathbb{H}_S(0)$, $\mathbb{G}_{SH0}(t) = \mathbb{G}_{SH}(0)$, $\mathbb{R}_{T0}(t) = \mathbb{R}_T(0)$, $\mathbb{R}_0(t) = \mathbb{R}(0)$. Using norm of the first equation from above, we get

$$\|\Phi_{1n}(t)\| = \|\mathbb{S}_n(t) - \mathbb{S}_{n-1}(t)\|,$$

$$\|\Phi_{1n}(t)\| = \left\| \frac{1}{\Gamma(\omega)}\int_0^t (t-x)^{\omega-1}(G_1(x,\mathbb{S}_{n-1}) - G_1(x,\mathbb{S}_{n-2}))dx \right\|,$$

$$\|\Phi_{1n}(t)\| \leqslant \frac{1}{\Gamma(\omega)}\left\| \int_0^t (t-x)^{\omega-1}(G_1(x,\mathbb{S}_{n-1}) - G_1(x,\mathbb{S}_{n-2}))dx \right\|.$$

By using Lipschiz condition we get

$$\|\mathbb{S}_n(t) - \mathbb{S}_{n-1}(t)\| \leqslant \frac{1}{\Gamma(\omega)}\mathfrak{L}_1\int_0^t (t-x)^{\omega-1}\|\mathbb{S}_{n-1} - \mathbb{S}_{n-2}\|\,dx.$$

This leads us to obtain (4.4)

$$\|\Phi_{1n}(t)\| \leqslant \frac{1}{\Gamma(\omega)}\mathfrak{L}_1\int_0^t (t-x)^{\omega-1}\left\|\Phi_{1(n-1)}(x)\right\|dx. \tag{4.4}$$

We can establish a similar equation for the other equation of the model (4.1) as follows in (4.5):

$$\begin{aligned}
&\|\Phi_{2n}(t)\| \leqslant \frac{1}{\Gamma(\omega)}\mathfrak{L}_2\int_0^t (t-x)^{\omega-1}\left\|\Phi_{2(n-1)}(x)\right\|dx, \quad \|\Phi_{3n}(t)\| \leqslant \frac{1}{\Gamma(\omega)}\mathfrak{L}_3\int_0^t (t-x)^{\omega-1}\left\|\Phi_{3(n-1)}(x)\right\|dx,\\
&\|\Phi_{4n}(t)\| \leqslant \frac{1}{\Gamma(\omega)}\mathfrak{L}_4\int_0^t (t-x)^{\omega-1}\left\|\Phi_{4(n-1)}(x)\right\|dx, \quad \|\Phi_{5n}(t)\| \leqslant \frac{1}{\Gamma(\omega)}\mathfrak{L}_5\int_0^t (t-x)^{\omega-1}\left\|\Phi_{5(n-1)}(x)\right\|dx,\\
&\|\Phi_{6n}(t)\| \leqslant \frac{1}{\Gamma(\omega)}\mathfrak{L}_6\int_0^t (t-x)^{\omega-1}\left\|\Phi_{6(n-1)}(x)\right\|dx, \quad \|\Phi_{7n}(t)\| \leqslant \frac{1}{\Gamma(\omega)}\mathfrak{L}_7\int_0^t (t-x)^{\omega-1}\left\|\Phi_{7(n-1)}(x)\right\|dx.
\end{aligned} \tag{4.5}$$

From above, we conclude

$$\begin{cases} \mathbb{S}_n(t) = \sum_{i=1}^{n} \Phi_{1i}(t), \\ \mathbb{U}_{Sn}(t) = \sum_{i=1}^{n} \Phi_{2i}(t), \\ \mathbb{U}_{Qn}(t) = \sum_{i=1}^{n} \Phi_{3i}(t), \\ \mathbb{H}_{Sn}(t) = \sum_{i=1}^{n} \Phi_{4i}(t), \\ \mathbb{G}_{SHn}(t) = \sum_{i=1}^{n} \Phi_{5i}(t), \\ \mathbb{R}_{Tn}(t) = \sum_{i=1}^{n} \Phi_{6i}(t), \\ \mathbb{R}_n(t) = \sum_{i=1}^{n} \Phi_{7i}(t). \end{cases}$$

We can now present the following result, which guarantees the uniqueness of the solution of the model (4.1).

Theorem 4.3. *The considered FO co-abuse system* (4.1) *has a unique solution, if* $\frac{1}{\Gamma(\omega)} b^{\omega} \mathfrak{L}_i < 1$, *for* $i = 1, 2, \ldots, 7$.

Proof. After verifying that the kernel properties hold, we can analyze (4.4) and (4.5) and use the recursive approach to obtain the following results given (4.6):

$$\begin{aligned} &\|\Phi_{1n}(t)\| \leqslant \|\mathbb{S}_0(t)\| \left[\frac{1}{\Gamma(\omega)} \mathfrak{L}_1 b^{\omega}\right]^n, \quad \|\Phi_{2n}(t)\| \leqslant \|\mathbb{U}_{S_0}(t)\| \left[\frac{1}{\Gamma(\omega)} \mathfrak{L}_2 b^{\omega}\right]^n, \\ &\|\Phi_{3n}(t)\| \leqslant \left\|\mathbb{U}_{Q_0}(t)\right\| \left[\frac{1}{\Gamma(\omega)} \mathfrak{L}_3 b^{\omega}\right]^n, \quad \|\Phi_{4n}(t)\| \leqslant \|\mathbb{H}_{S_0}(t)\| \left[\frac{1}{\Gamma(\omega)} \mathfrak{L}_4 b^{\omega}\right]^n, \\ &\|\Phi_{5n}(t)\| \leqslant \|\mathbb{G}_{SH_0}(t)\| \left[\frac{1}{\Gamma(\omega)} \mathfrak{L}_5 b^{\omega}\right]^n, \quad \|\Phi_{6n}(t)\| \leqslant \|\mathbb{R}_{T_0}(t)\| \left[\frac{1}{\Gamma(\omega)} \mathfrak{L}_6 b^{\omega}\right]^n, \\ &\|\Phi_{7n}(t)\| \leqslant \|\mathbb{R}_0(t)\| \left[\frac{1}{\Gamma(\omega)} \mathfrak{L}_7 b^{\omega}\right]^n. \end{aligned} \tag{4.6}$$

It follows that $\|\Phi_{1n}(t)\| \to \infty$, $\|\Phi_{2n}(t)\| \to \infty$, $\|\Phi_{3n}(t)\| \to \infty$, $\|\Phi_{4n}(t)\| \to \infty$, $\|\Phi_{5n}(t)\| \to \infty$, $\|\Phi_{6n}(t)\| \to \infty$, $\|\Phi_{7n}(t)\| \to \infty$. Furthermore, from equation (4.6) and by applying the triangle inequality, we obtain

$$\begin{aligned} &\|\mathbb{S}_{n+c}(t) - \mathbb{S}_n(t)\| \leqslant \sum_{k=n+1}^{n+c} B_1^k = \frac{B_1^{n+1} - B_1^{n+c+1}}{1 - B_1}, \quad \|\mathbb{U}_{Sn+c}(t) - \mathbb{U}_{Sn}(t)\| \leqslant \sum_{k=n+1}^{n+c} B_2^k = \frac{B_2^{n+1} - B_2^{n+c+1}}{1 - B_2}, \\ &\left\|\mathbb{U}_{Qn+c}(t) - \mathbb{U}_{Qn}(t)\right\| \leqslant \sum_{k=n+1}^{n+c} B_3^k = \frac{B_3^{n+1} - B_3^{n+c+1}}{1 - B_3}, \quad \|\mathbb{H}_{Sn+c}(t) - \mathbb{H}_{Sn}(t)\| \leqslant \sum_{k=n+1}^{n+c} B_4^k = \frac{B_4^{n+1} - B_4^{n+c+1}}{1 - B_4}, \\ &\|\mathbb{G}_{SHn+c}(t) - \mathbb{G}_{SHn}(t)\| \leqslant \sum_{k=n+1}^{n+c} B_5^k = \frac{B_5^{n+1} - B_5^{n+c+1}}{1 - B_5}, \quad \|\mathbb{R}_{Tn+c}(t) - \mathbb{R}_{Tn}(t)\| \leqslant \sum_{k=n+1}^{n+c} B_6^k = \frac{B_6^{n+1} - B_6^{n+c+1}}{1 - B_6}, \\ &\|\mathbb{R}_{n+c}(t) - \mathbb{R}_n(t)\| \leqslant \sum_{k=n+1}^{n+c} B_7^k = \frac{B_7^{n+1} - B_7^{n+c+1}}{1 - B_7}, \end{aligned} \tag{4.7}$$

where $\frac{1}{\Gamma(\omega)} b^{\omega} \mathfrak{L}_i < 1$, by assertion and $B_i = \left[\frac{1}{\Gamma(\omega)} \mathfrak{L}_i b^{\omega}\right]^n$, for $i = 1, 2, \ldots, 7$. Therefore, $\mathbb{S}_n$, $\mathbb{U}_{Sn}$, $\mathbb{U}_{Qn}$, $\mathbb{H}_{Sn}$, $\mathbb{G}_{SHn}$, $\mathbb{R}_{Tn}$, $\mathbb{R}_n$ are used as the cauchy sequence in $G(J)$. Thus, we have shown that the sequences are uniformly convergent, as stated in [10]. By applying limit theory to (4.7)) as n approaches infinity, we can conclude that the limit of these sequences is the unique solution of the model (3.1). □

4.5. Ulam-Hyers stability

In this portion, we discuss the different types of Ulam Hyers (UH) stability (UHS). The definitions of different Ulam Hyers stabilizes for our proposed system. Let $q > 0$ and $\mathfrak{I}_Z : [0, \mathcal{T}] \times \mathbb{R}^7 \to \mathbb{R}^+$ shows a continuous function. Consider the inequalities given by:

$$\left|{}^{C}\mathcal{D}_t^{\omega} \mathbb{V}(t) - \mathbb{W}(t, \mathbb{V}(t))\right| \leqslant q, \tag{4.8}$$

$$\begin{aligned} \left|{}^{C}\mathcal{D}_{t}^{\omega}\mathbb{V}(t)-\mathbb{W}(t,\mathbb{V}(t))\right| &\leqslant q\mathfrak{I}_{Z}(t), \\ \left|{}^{C}\mathcal{D}_{t}^{\omega}\mathbb{V}(t)-\mathbb{W}(t,\mathbb{V}(t))\right| &\leqslant \mathfrak{I}_{Z}(t). \end{aligned} \tag{4.9}$$

where $t \in [0,\mathcal{T}]$ and $\vartheta = \max(\vartheta_i)^{\mathcal{T}}$, for $i = 1,2,\ldots,7$.

Definition 4.4. The proposed system will become (UHS) if for every $q > 0$, and for every solution $\mathbb{V} \in \mathbb{B}$ of (4.8), $\exists \mathfrak{I}_Z > 0$ and a solution $\mathbb{Q} \in \mathbb{B}$ with $|\mathbb{V}(t)-\mathbb{Q}(t)| \leqslant q\mathfrak{I}_Z > 0$, where $\mathfrak{I}_Z = \max(\mathfrak{I}_{Z_i})^{\mathcal{T}}$ for $i = 1,2,\ldots,7$.

Definition 4.5. The proposed system will be generalized (UHS) if $\exists$ a function $\mathfrak{I}_Z$ with $\mathfrak{I}_{\mathbb{Z}}(0) = 0$, $|\mathbb{V}(t)-\mathbb{Q}(t)| \leqslant \mathfrak{I}_Z(\vartheta)$, where $\mathfrak{I}_Z = \max(\mathfrak{I}_{Z_i})^{\mathcal{T}}$ for $i = 1,2,\ldots,7$.

Definition 4.6. The considered FO co-abuse will be UHRS if $\exists\ \mathbb{U}_{\mathfrak{I}_Z} > 0$ so that $|\mathbb{V}(t)-\mathbb{Q}(t)| \leqslant \mathfrak{I}_Z(t)\mathbb{U}_{\mathfrak{I}_Z}q$.

Definition 4.7. The proposed model is generalized (UHR) if $\exists\ \mathbb{U}_{\mathfrak{I}_Z} > 0$, such that $|\mathbb{V}(t)-\mathbb{Q}(t)| \leqslant \mathfrak{I}_Z(t)\mathbb{U}_{\mathfrak{I}_Z}$.

Remark 4.8. Let $\mathbb{V} \in \mathbb{B}$ be a solution of (4.9) iff there exists $H \in \mathbb{B}$, that possesses the assertions given as:

- $|H(t)| \leqslant \vartheta, \mathfrak{I}_Z(t),\ H = \max(H_i)^{\mathsf{T}}$, for $i = 1,2,\ldots,7$.
- ${}^{c}D_{t}^{\omega}\mathbb{V}(t) = \mathbb{W}(t,\mathbb{V}(t)+H(t)$.

To aid our exploration of Ulam's stabilities concerning the suggested model, we'll initially establish certain essential outcomes. Moreover, we introduce an assumption that may be beneficial for our subsequent analysis. We shall assume that:

(B_3) $\forall\ t \in [0,T]$, $\exists$ an increasing function $\mathfrak{I}_Z \in \mathbb{B}$ and $\Omega_{\mathfrak{I}_Z} > 0$, so that ${}^{c}\mathfrak{I}_{0}^{\omega}\mathfrak{I}_Z(t) \leqslant \Omega_{\mathfrak{I}_Z}\mathfrak{I}_Z(t)$.

Lemma 4.9. *For* $\mathbb{V} \in \mathbb{B}$, *the following inequality holds:*

$$\left|\mathbb{V}(t)-\mathbb{V}_0-\frac{1}{\Gamma(\omega)}\int_0^t (t-x)^{\omega-1}\mathbb{Z}(x,\mathbb{V}(x))dx\right| \leqslant \frac{\sigma t^{\omega}}{\Gamma(\omega+1)}.$$

Proof. Since $\mathbb{V} \in \mathbb{B}$ satisfies (4.8). Hence, using second portion of Remark 4.8, one reaches

$$\begin{cases} {}^{c}D_{t}^{\omega}\mathbb{V}(t) = \mathbb{W}(t,\mathbb{V}(t)) + G(t),\ t \in [0,\mathcal{T}], \\ \mathbb{V}(0) = \mathbb{V}_0. \end{cases} \tag{4.10}$$

By using the fractional integral, we get the solution of (4.10) and is expressed as:

$$V(t) = \mathbb{V}_0 + \frac{1}{\Gamma(\omega)}\int_0^t (t-x)^{\omega-1}\mathbb{W}(x,\mathbb{V}(x))dx + \frac{1}{\Gamma(\omega)}\int_0^t (t-x)^{\omega-1}G(x)dx.$$

Given the initial assumption, employing the initial segment of Remark 4.8 enables us to derive the subsequent result:

$$\begin{aligned} &\left|\mathbb{V}(t)-\mathbb{V}_0-\frac{1}{\Gamma(\omega)}\int_0^t (t-x)^{\omega-1}\mathbb{W}(x,\mathbb{V}(x))dx\right| \\ &= \left|\frac{1}{\Gamma(\omega)}\int_0^t (t-x)^{\omega-1}G(x)dx\right| \leqslant \frac{1}{\Gamma(\omega)}\int_0^t (t-x)^{\omega-1}|G(x)|\,dx \leqslant \frac{\sigma t^{\omega}}{\Gamma(\omega+1)}. \end{aligned}$$

Hence, which is proved. □

Lemma 4.10. *Let* $\mathbb{V} \in \mathbb{B}$ *satisfies* (4.9), *then*

$$\left|\mathbb{V}(t)-\mathbb{V}_0-\frac{1}{\Gamma(\omega)}\int_0^t (t-x)^{\omega-1}\mathbb{W}(x,\mathbb{V}(x))dx\right| \leqslant \omega\Omega_{\mathfrak{I}_Z}\mathfrak{I}_Z(t).$$

Proof. Since $\mathbb{V} \in \mathbb{B}$ is a solution of (4.8), given the 2nd portion of Remark 4.8, it can be represented as follows:

$$\mathbb{V}(t) = \mathbb{V}_0 + \frac{1}{\Gamma(\omega)} \int_0^t (t-x)^{\omega-1} \mathbb{W}(x, \mathbb{V}(x)) dx + \frac{1}{\Gamma(\omega)} \int_0^t (t-x)^{\omega-1} H(x) dx.$$

Referring to the initial segment of Remark 4.8, we express the aforementioned equation:

$$|\mathbb{V}(t) - \mathbb{V}_0 - {}^c\mathcal{I}_0^{\omega} \mathbb{W}(x, \mathbb{V}(x))| = |{}^c\mathcal{I}_0^{\omega} H(t)| \leqslant {}^c\ \mathcal{I}_0^{\omega} |H(t)| \leqslant \sigma {}^c\mathcal{I}_0^{\omega} \mathfrak{I}_Z(t) \leqslant \sigma \Omega \mathfrak{I}_Z(t).$$

□

We are now ready to validate the Ulam-Hyers (UH) and Ulam-Hyers-Rassias (UHR) stability of the proposed co-abuse system.

Theorem 4.11. *Inview of assumption* (B_1)*, and if* $\frac{\Re_Z \mathcal{T}^{\omega}}{\Gamma(\omega+1)} < 1$*, hold, then the solution of* (4.2) *UH and generalized UH stable.*

Proof. Let $q > 0$ and $\mathbb{V} \in \mathbb{B}$ is any solution of (4.8). Let $\mathbb{Q} \in \mathbb{B}$ denote unique solution for the model (4.2). Utilizing (4.3) and Lemma 4.1, one gets

$$\begin{aligned}
|\mathbb{V}(t) - \mathbb{Q}(t)| &\leqslant \left| \mathbb{V}(t) - \mathbb{Q}_0 - \frac{1}{\Gamma(\omega)} \int_0^t (t-x)^{\omega-1} \mathbb{W}(x, \mathbb{Q}(x)) dx \right| \\
&\leqslant \left| \mathbb{V}(t) - \mathbb{V}_0 - \frac{1}{\Gamma(\omega)} \int_0^t (t-x)^{\omega-1} \mathbb{W}(x, \mathbb{Q}(x)) dx \right| \\
&\quad \dot{+} \frac{1}{\Gamma(\omega)} \int_0^t (t-x)^{\omega-1} |\mathbb{W}(x, \mathbb{V}(x)) - \mathbb{W}(x, \mathbb{Q}(x))| \, dx \\
&\leqslant \left| \mathbb{V}(t) - \mathbb{V}_0 - \frac{1}{\Gamma(\omega)} \int_0^t (t-x)^{\omega-1} \mathbb{W}(x, \mathbb{Q}(x)) dx \right| \dot{+} \frac{\Re_Z}{\Gamma(\omega)} \int_0^t (t-x)^{\omega-1} |\mathbb{V}(x) - \mathbb{Q}(x)| \, dx \\
&\leqslant \frac{\sigma t^{\omega}}{\Gamma(\omega+1)} + \frac{\Re_Z \mathcal{T}^{\omega}}{\Gamma(\omega+1)} |\mathbb{V}(t) - \mathbb{Q}(t)|.
\end{aligned}$$

Through a series of computations, we obtain $|\mathbb{V}(t) - \mathbb{Q}(t)| \leqslant q \mathscr{J}_Z$, where

$$\mathscr{J}_Z = \frac{\frac{t^{\omega}}{\Gamma(\omega+1)}}{1 - \frac{\Re_Z \mathcal{T}^{\omega}}{\Gamma(\omega+1)}}.$$

Hence, the result of UHS is obtained. Therefore, the FO co-abuse system (4.2) is UHS. Next, set $\mathfrak{I}_Z(\sigma) = \sigma \mathcal{J}$ so that $\mathfrak{I}_Z(0) = 0$. Thus, the FO co-abuse model is generalized (UHS). □

The provided system demonstrates Ulam-Hyers-Rassias stability (UHRS) and generalized Ulam-Hyers-Rassias stability (UHRS) based on the following theorem.

Theorem 4.12. *Under the assumptions* (B_1), (B_3)*, and if* $\frac{\Re_Z \mathcal{T}^{\omega}}{\Gamma(\omega+1)} < 1$ *hold, then the model*(4.2) *solution is UHRS and generalized UHRS.*

Proof. Via Lemma 4.9, one gets

$$\begin{aligned}
|\mathbb{V}(t) - \mathbb{Q}(t)| &\leqslant \left| \mathbb{V}(t) - \mathbb{Q}_0 - \frac{1}{\Gamma(\omega)} \int_0^t (t-x)^{\omega-1} \mathbb{W}(x, \mathbb{Q}(x)) dx \right| \\
&\leqslant \left| \mathbb{V}(t) - \mathbb{V}_0 - \frac{1}{\Gamma(\omega)} \int_0^t (t-x)^{\omega-1} \mathbb{W}(x, \mathbb{Q}(x)) dx \right|
\end{aligned}$$

$$
\begin{aligned}
&\dot{+}\,\frac{1}{\Gamma(\omega)}\int_0^t (t-x)^{\omega-1}\,|\mathbb{W}(x,\mathbb{V}(x))-\mathbb{W}(x,\mathbb{Q}(x))|\,dx\\
&\leqslant \left|\mathbb{V}(t)-\mathbb{V}_0-\frac{1}{\Gamma(\omega)}\int_0^t (t-x)^{\omega-1}\,\mathbb{W}(x,\mathbb{Q}(x))dx\right| \dot{+}\,\frac{\Re_Z}{\Gamma(\omega)}\int_0^t (t-x)^{\omega-1}\,|\mathbb{V}(x)-\mathbb{Q}(x)|\,dx\\
&\leqslant \sigma\Omega_{\mathfrak{I}_Z}\mathfrak{I}_Z(t)+\frac{\Re_Z\mathcal{T}^{\omega}}{\Gamma(\omega+1)}\,|\mathbb{V}(t)-\mathbb{Q}(t)|\,.
\end{aligned}
$$

After simplification, one acquires $|\mathbb{V}(t)-\mathbb{Q}(t)|\leqslant \frac{\sigma\Omega_{\mathfrak{I}_Z}\mathfrak{I}_Z(t)}{1-\frac{\Re_Z\mathcal{T}^{\omega}}{\Gamma(\omega+1)}}$. Supposing

$$
\mathbb{U}_{\mathfrak{I}_Z}=\frac{\Omega_{\mathfrak{I}_Z}}{1-\frac{\Re_Z\mathcal{T}^{\omega}}{\Gamma(\omega+1)}},
$$

we get our result:

$$
|\mathbb{V}(t)-\mathbb{Q}(t)|\leqslant \mathfrak{I}_Z(t)\Omega_{\mathfrak{I}_Z}. \tag{4.11}
$$

Consequently, the proposed model is UHR stable. Then, by setting $\sigma=1$ in (4.11) along with $\mathfrak{I}_Z(0)=0$, the proposed model is generalized UHR stable. □

5. Numerical outcomes of Co-abuse model through Euler method

The task of realizing exact solutions to systems of (FO) differential equations leftovers a challenging problem in numerical and mathematical modeling. In this segment, we present a methodology for obtaining estimated solutions to fractional order systems. We will employ a numerical fractional Euler's method. We will explain the algorithm for the fractional Euler's numerical solution method. Take a general FO differential equation as given in (5.1):

$$
{}^{C}\mathcal{D}_t^{\omega}\mathbb{X}(t)=L\left(t,\mathbb{X}\left(t\right)\right),\quad a\leqslant t\leqslant q, \tag{5.1}
$$

$\mathbb{S}(t)=c$, where $a=t_0,t_1,\ldots,t_n=q$ such that $t_j=c+j\nabla$. Let $i=0,1,2,\ldots,n$, and $\nabla=\frac{q-a}{n}$. Assume that ${}^{C}\mathcal{D}_t^{\omega}\mathbb{X}(t)$ and ${}^{C}\mathcal{D}_t^{2\omega}\mathbb{X}(t)$ are continuous functions on $[a,q]$. Via Taylor's expansion, one gets

$$
\mathbb{X}\left(t_{j+1}\right)=\mathbb{X}\left(t_j+\nabla\right)=\mathbb{X}\left(t_j\right)+\frac{\nabla^{\omega}}{\omega}\left({}^{C}\mathcal{D}_t^{\omega}\mathbb{X}(t_j)\right)+\frac{\nabla^{2\omega}}{2\omega^2}\left({}^{C}\mathcal{D}_t^{2\omega}\mathbb{X}\right)\left(v_i\right),
$$

where $t_j<v_j<t_{j+1}$. Since $\nabla=t_{j+1}-t_j$, there exists $\Theta_j\epsilon\,(0,1)$ such that

$$
\mathbb{X}\left(t_{j+1}\right)=\mathbb{X}\left(t_j\right)+\frac{\nabla^{\omega}}{\omega}\left({}^{C}\mathcal{D}_t^{\omega}\mathbb{X}(t_j)\right)+\frac{\nabla^{2\omega}}{2\omega^2}\left({}^{C}\mathcal{D}_t^{2\omega}\mathbb{X}\right)\left(t_j+\Theta_j\nabla\right),
$$

from which we have

$$
\frac{\omega\left(\mathbb{X}(t_{j+1})-\mathbb{X}(t_j)\right)}{\nabla^{\omega}}=L\left(t_j,\mathbb{X}(t_j)\right)+\frac{\nabla^{2\omega}}{2\omega^2}\left({}^{C}\mathcal{D}_t^{2\omega}\mathbb{X}\right)\left(t_j+\Theta_j\nabla\right). \tag{5.2}
$$

For a sufficiently brief time interval, ∇, the term $\frac{\nabla^{2\omega}}{2\omega^2}\left({}^{C}\mathcal{D}_t^{2\omega}\mathbb{X}\right)\left(t_j+\Theta_j\nabla\right)$in (5.2) could be neglected. So, from (5.2), the numerical technique is derived in the following format:

$$
\mathbb{X}\left(t_{j+1}\right)=\mathbb{X}\left(t_j\right)+\frac{\nabla^{\omega}}{\omega}L\left(t_j,\mathbb{X}(t_j)\right). \tag{5.3}
$$

Agarwal et al. employed Euler's methods within their paper [20] to devise a comparable numerical scheme, offering a solution for (5.1) as

$$
\mathbb{X}\left(t_{j+1}\right)=\mathbb{X}\left(t_j\right)+\frac{\nabla^{\omega}}{\Gamma\left(\omega+1\right)}L\left(t_j,\mathbb{X}(t_j)\right). \tag{5.4}
$$

The discrete (5.3) and (5.4) only differ in denominator on right sides. In this work, we bring the numerical technique expressed in (5.3) and employ the earlier scheme for ease of computation. We employ the numerical estimation scheme (5.4). First we take the equation

$$^{C}\mathcal{D}_{t}^{\omega}\mathbb{S}(t) = \Lambda - \beta_1\Pi_1\mathbb{S} - \beta_2\Pi_2\mathbb{S} - \mu\mathbb{S},$$

for $0 < \omega < 1$, $t > 0$, with initial values $\mathbb{S}(0)=\mathbb{S}^0 = 500$, $\mathbb{U}_S(0) = \mathbb{U}_S^0 = 200$, $\mathbb{U}_Q(0) = \mathbb{U}_Q^0 = 100$, $\mathbb{H}_S(0) = \mathbb{H}_S^0 = 100$, $\mathbb{G}_{SH}(0) = \mathbb{G}_{SH}^0 = 100$, $\mathbb{R}_T(0) = \mathbb{R}_T^0 = 0$, $\mathbb{R}(0) = \mathbb{R}^0 = 0$, and the total population $\mathbb{N} = 1000$. Suppose $L(t,\mathbb{S}(t)) = \Lambda - \beta_1\Pi_1\mathbb{S} - \beta_2\Pi_2\mathbb{S} - \mu\mathbb{S}$, so we define $^{C}\mathcal{D}_{t}^{\omega}\mathbb{S}(t) = L(t,\mathbb{S}(t))$ with $\mathbb{S}_0 = 500$. Next, by applying the numerical schema expressed at (5.4), one has

$$\mathbb{X}\left(t_{j+1}\right) = \mathbb{X}\left(t_j\right) + \frac{\nabla^{\omega}}{\Gamma(\omega+1)} L\left(t_j,\mathbb{S}(t_j)\right),$$

where $L\left(t_j,\mathbb{S}(t_j)\right)$ is expressed by

$$L\left(t_j,\mathbb{S}(t_j)\right) = \Lambda - \beta_1\Pi_1\mathbb{S}(t_j) - \beta_2\Pi_2\mathbb{S}(t_j) - \mu\mathbb{S}(t_j),$$

for $j = 0,1,2,3,\ldots,n-1$. Now,

$$^{C}\mathcal{D}_{t}^{\omega}\mathbb{U}_S(t) = \beta_1\Pi_1\mathbb{S}(t) + \delta_2\mathbb{G}_{SH}(t) + \xi_2\mathbb{R}_T(t) + \rho_1\mathbb{U}_Q(t) - \gamma_1\mathbb{U}_S(t) - (\tau_1+\rho_1+\mu)\mathbb{U}_S(t).$$

Let

$$L(t,\mathbb{U}_S(t)) = \beta_1\Pi_1\mathbb{S}(t) + \delta_2\mathbb{G}_{SH}(t) + \xi_2\mathbb{R}_T(t) + \rho_1\mathbb{U}_Q(t) - \gamma_1\mathbb{U}_S(t) - (\tau_1+\rho_1+\mu)\mathbb{U}_S(t),$$

then we define $^{C}\mathcal{D}_{t}^{\omega}\mathbb{U}_S(t) = L(t,\mathbb{U}_S(t))$ with $\mathbb{U}_{S0} = 200$. Hence, applying the numerical schema outlined in (5.4), we have

$$\mathbb{U}_S\left(t_{j+1}\right) = \mathbb{U}_S\left(t_j\right) + \frac{\nabla^{\omega}}{\Gamma(\omega+1)} L\left(t_j,\mathbb{U}_S(t_j)\right),$$

where $L\left(t_j,\mathbb{U}_S(t_j)\right)$ is expressed by

$$L\left(t_j,\mathbb{U}_S(t_j)\right) = \beta_1\Pi_1\mathbb{S}(t) + \delta_2\mathbb{G}_{SH}(t) + \xi_2\mathbb{R}_T(t) + \rho_1\mathbb{U}_Q(t) - \gamma_1\mathbb{U}_S(t) - (\tau_1+\rho_1+\mu)\mathbb{U}_S(t),$$

for $j = 0,1,2,3,\ldots,n-1$. Next,

$$^{C}\mathcal{D}_{t}^{\omega}\mathbb{U}_Q(t) = \tau_1\mathbb{U}_S(t) - (\rho_1+\mu)\mathbb{U}_Q(t).$$

Let us suppose

$$L\left(t,\mathbb{U}_Q(t)\right) = \tau_1\mathbb{U}_S(t) - (\rho_1+\mu)\mathbb{U}_Q(t).$$

Next, we establish $^{C}\mathcal{D}_{t}^{\omega}\mathbb{U}_Q(t) = L\left(t,\mathbb{U}_Q(t)\right)$ with $\mathbb{U}_{Q0} = 100$. Hence, putting on the numerical schema outlined in (5.4), we have

$$\mathbb{U}_Q\left(t_{j+1}\right) = \mathbb{U}_Q\left(t_j\right) + \frac{\nabla^{\omega}}{\Gamma(\omega+1)} L\left(t_j,\mathbb{U}_Q(t_j)\right),$$

where $L\left(t_j,\mathbb{U}_Q(t_j)\right)$ is expressed by

$$L\left(t_j,\mathbb{U}_Q(t_j)\right) = \tau_1\mathbb{U}_S(t) - (\rho_1+\mu)\mathbb{U}_Q(t),$$

for $j = 0,1,2,3,\ldots,n-1$. Let us consider

$$^{C}\mathcal{D}_{t}^{\omega}\mathbb{H}_S(t) = \beta_2\Pi_2\mathbb{S}(t) + \delta_1\mathbb{G}_{SH}(t) + \xi_3\mathbb{R}_T(t) + \rho_2\mathbb{R}(t) - \gamma_2\Pi_2\mathbb{H}_S(t) - (\tau_2+\rho_2+\mu)\mathbb{H}_S(t).$$

Let

$$L(t, \mathbb{H}_S(t)) = \beta_2\Pi_2\mathbb{S}(t) + \delta_1\mathbb{G}_{SH}(t) + \xi_3\mathbb{R}_T(t) + \rho_2\mathbb{R}(t) - \gamma_2\Pi_2\mathbb{H}_S(t) - (\tau_2 + \rho_2 + \mu)\mathbb{H}_S(t).$$

Next, we establish ${}^{C}\mathcal{D}_t^{\omega}\mathbb{H}_S(t) = L(t, \mathbb{H}_S(t))$ with $\mathbb{H}_{S0} = 100$. Hence, putting on the numerical solution scheme outlined in (5.4), we have

$$\mathbb{H}_S\left(t_{j+1}\right) = \mathbb{H}_S\left(t_j\right) + \frac{\nabla^{\omega}}{\Gamma(\omega+1)} L\left(t_j, \mathbb{H}_S(t_j)\right),$$

where $L\left(t_j, \mathbb{H}_S(t_j)\right)$ is expressed by

$$L\left(t_j, \mathbb{H}_S(t_j)\right) = \beta_2\Pi_2\mathbb{S}(t) + \delta_1\mathbb{G}_{SH}(t) + \xi_3\mathbb{R}_T(t) + \rho_2\mathbb{R}(t) - \gamma_2\Pi_2\mathbb{H}_S(t) - (\tau_2 + \rho_2 + \mu)\mathbb{H}_S(t),$$

for $j = 0, 1, 2, 3, \ldots, n-1$. Now,

$${}^{C}\mathcal{D}_t^{\omega}\mathbb{G}_{SH}(t) = \gamma_1\Pi_1\mathbb{U}_S(t) + \gamma_2\Pi_2\mathbb{H}_S(t) + \xi_1\mathbb{R}_T(t) - (\kappa_2 + \delta + \delta_1 + \delta_2 + \rho_3 + \mu)\mathbb{G}_{SH}(t).$$

Consider

$$L(t, \mathbb{G}_{SH}(t)) = \gamma_1\Pi_1\mathbb{U}_S(t) + \gamma_2\Pi_2\mathbb{H}_S(t) + \xi_1\mathbb{R}_T(t) - (\kappa_2 + \delta + \delta_1 + \delta_2 + \rho_3 + \mu)\mathbb{G}_{SH}(t),$$

then we define ${}^{C}\mathcal{D}_t^{\omega}\mathbb{G}_{SH}(t) = L(t, \mathbb{G}_{SH}(t))$ with $\mathbb{G}_{SH0} = 100$. Hence, by utilizing the numerical solution scheme outlined in (5.4), we have

$$\mathbb{G}_{SH}\left(t_{j+1}\right) = \mathbb{G}_{SH}\left(t_j\right) + \frac{\nabla^{\omega}}{\Gamma(\omega+1)} L\left(t_j, \mathbb{G}_{SH}(t_j)\right),$$

where $L\left(t_j, \mathbb{G}_{SH}(t_j)\right)$ is expressed by

$$L\left(t_j, \mathbb{G}_{SH}(t_j)\right) = \gamma_1\Pi_1\mathbb{U}_S(t) + \gamma_2\Pi_2\mathbb{H}_S(t) + \xi_1\mathbb{R}_T(t) - (\kappa_2 + \delta + \delta_1 + \delta_2 + \rho_3 + \mu)\mathbb{G}_{SH}(t),$$

for $j = 0, 1, 2, 3, \ldots, n-1$. Next,

$${}^{C}\mathcal{D}_t^{\omega}\mathbb{R}_T(t) = \tau_2\mathbb{H}_S(t) + \delta\mathbb{G}_{SH}(t) - (\kappa_3 + \xi + \xi_2 + \xi_3 + \mu)\mathbb{R}_T(t).$$

Assume

$$L(t, \mathbb{R}_T(t)) = \tau_2\mathbb{H}_S(t) + \delta\mathbb{G}_{SH}(t) - (\kappa_3 + \xi + \xi_2 + \xi_3 + \mu)\mathbb{R}_T(t),$$

then we define ${}^{C}\mathcal{D}_t^{\omega}\mathbb{R}_T(t) = L(t, \mathbb{R}_T(t))$ with $\mathbb{R}_{T0} = 0$. Hence, utilizing the numerical solution scheme outlined in (5.4), we have

$$\mathbb{R}_T\left(t_{j+1}\right) = \mathbb{R}_T\left(t_j\right) + \frac{\nabla^{\omega}}{\Gamma(\omega+1)} L\left(t_j, \mathbb{R}_T(t_j)\right),$$

where $L\left(t_j, \mathbb{G}_{SH}(t_j)\right)$ is expressed by

$$L\left(t_j, \mathbb{R}_T(t_j)\right) = \tau_2\mathbb{H}_S(t) + \delta\mathbb{G}_{SH}(t) - (\kappa_3 + \xi + \xi_2 + \xi_3 + \mu)\mathbb{R}_T(t),$$

for $j = 0, 1, 2, 3, \ldots, n-1$. At the end, we consider

$${}^{C}\mathcal{D}_t^{\omega}\mathbb{R}(t) = \kappa_2\mathbb{G}_{SH}(t) + \kappa_3\mathbb{R}_T(t) - (\rho_2 + \mu)\mathbb{R}(t).$$

Let

$$L(t, \mathbb{R}(t)) = \kappa_2\mathbb{G}_{SH}(t) + \kappa_3\mathbb{R}_T(t) - (\rho_2 + \mu)\mathbb{R}(t).$$

Next, we establish ${}^{C}\mathcal{D}_t^{\omega}\mathbb{R}(t) = L(t, \mathbb{R}(t))$ with $\mathbb{R}_0 = 0$. Hence, putting on the numerical schema in (5.4), we have

$$\mathbb{R}\left(t_{j+1}\right) = \mathbb{R}\left(t_j\right) + \frac{\nabla^{\omega}}{\Gamma(\omega+1)} L\left(t_j, \mathbb{R}(t_j)\right),$$

where $L\left(t_j, \mathbb{G}_{SH}(t_j)\right)$ is expressed by

$$L\left(t_j, \mathbb{R}(t_j)\right) = \kappa_2\mathbb{G}_{SH}(t) + \kappa_3\mathbb{R}_T(t) - (\rho_2 + \mu)\mathbb{R}(t),$$

for $j = 0, 1, 2, 3, \ldots, n-1$.

6. Numerical simulations and discussion

In this part, we are going to depict the numerical results obtained via Euler numerical method. For the simulation, we take initial values as: $\mathbb{S}(0) = 500$, $\mathbb{U}_S(0) = 200$, $\mathbb{U}_Q(0) = 100$, $\mathbb{H}_S(0) = 100$, $\mathbb{G}_S\mathbb{H}(0) = 100$, $\mathbb{R}_t(0) = 0$, $\mathbb{R}(0) = 0$. Also, the values of parameters are $\Lambda = 5$, $\beta_1 = 1$, $\beta_2 = 0.2$, $\varpi_1 = 0.8$, $\varpi_2 = 0.2$, $\xi_1 = 0.4$, $\xi_2 = 0.3$, $\xi_3 = 0.6$, $\mu = 0.0002$, $\gamma_1 = 2.5$, $\gamma_2 = 2$, $\tau_1 = 0.001$, $\tau_2 = 0.3$, $\kappa_2 = 0.3$, $\kappa_3 = 0.9$, $\delta = 0.3$, $\delta_1 = 0.5$, $\delta_2 = 0.35$, $\rho_1 = 0.03$, $\rho_2 = 0.0033$, $\rho_3 = 0.04$, $\epsilon_1 = 1.05$, $\epsilon_2 = 0.7$, $\epsilon_3 = 1.05$, $\epsilon_4 = 0.7$, $\mathbb{N} = 1000$. The figures displaying the compartments of the co-abuse system are presented in Figures 2 and 3. In Figure 2, the first four compartments of the system are visualized based on the considered parameters and initial values. In Figure 2 (a), the figure reveals a decrease in the number of susceptible individuals over time. This decrease can be attributed to their interaction with people who are smoking. In Figure 2 (b), the figure reveals an increase over time due to the absence of government intervention or treatment options. In Figure 2 (c), the number of individuals who quit smoking also declines due to a lack of restrictions and treatment options. In Figure 2 (d), the figure reveals an increase over time due to the absence of government intervention or treatment options.

Furthermore, Figure 3 displays the dynamics of the last three compartments of the system for considered parameters and initial values. In Figure 3 (a), it can be observed that the number of co-abuse individuals increases over time due to the absence of government intervention or treatment options. In Figure 3 (b), if smoking and heroin treatment options are implemented, the number of co-abuse treatments increases, leading to a higher number of recovered individuals from both smoking and heroin addiction. Finally, Figure 3 (b) shows that more addicted co-abuse individuals will be able to recover.

Additionally, all the graphs are simulated for some fractional orders to observe the memory features of the considered system. It's important to highlight that the model achieves stability more quickly at lower fractional orders in contrast to higher orders. Additionally, as the fractional order increases, the graphs of each class tend to converge towards the dynamics of the classical model. Consequently, we can infer that the suggested model is more advanced and encompasses a broader range of applications compared to the classical model.

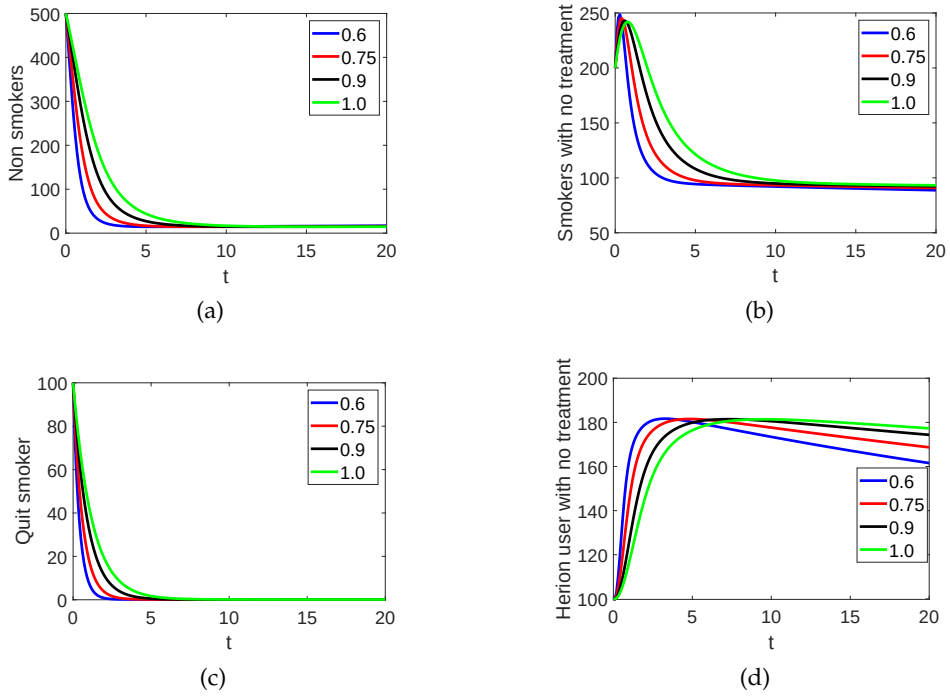

Figure 2: Graphs of the proposed system for first four classes.

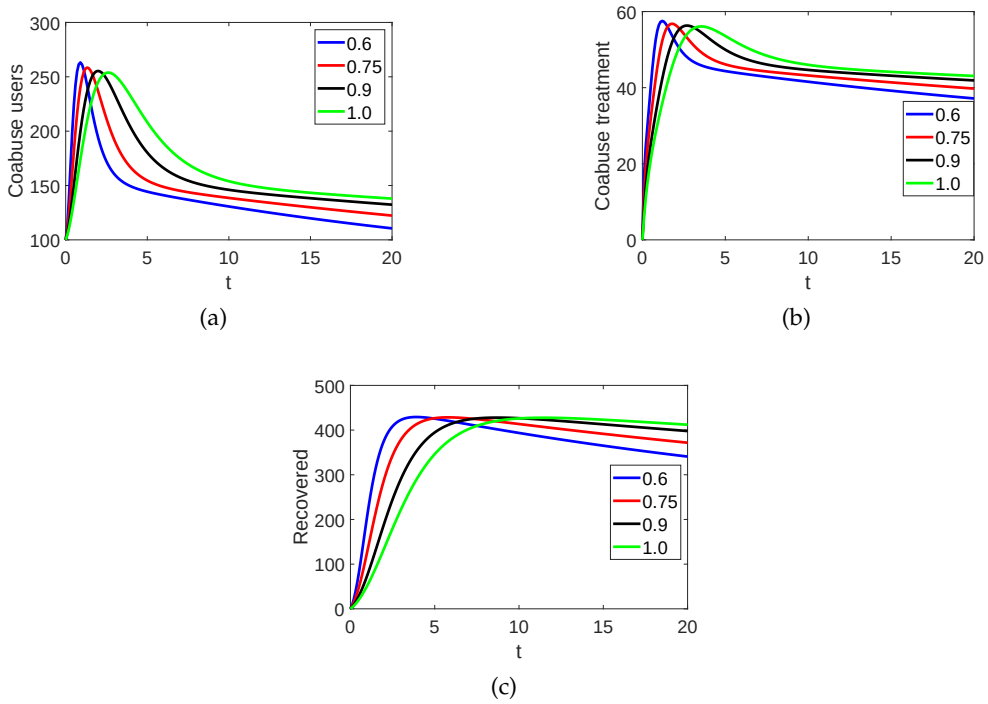

Figure 3: Graphs of the last three classes.

7. Conclusion

In our study, we introduced a mathematical model that aimed to demonstrate the co-abuse infection of smoking and heroin. In order to demonstrate solutions that are not negative and to define a stable equilibrium point and a fundamental reproductive number, we broadened the model by incorporating Caputo fractional-order (FO) derivative operators. We used functional analysis concepts to develop some results related to the presence of a solitary solution. Furthermore, we utilized the Ulam-Hyers (UH) concept to showcase the stability of the model's solution. To provide additional insight, we showcased numerical results for the (FO) system using an helpful Euler-type numerical approach. These results were depicted in graphs, which demonstrated the varied reactions of the considered system for different parameter values.

Through our analysis, we were able to observe the impact of the different variables on the system's dynamics and gain a better understanding of the model's behavior. By utilizing the numerical results, we made informed conclusions about the co-abuse infection of smoking and heroin. Overall, the study provided valuable insights into the co-abuse infection of smoking and heroin and demonstrated the usefulness of mathematical modeling for understanding complex systems. A complex system refers to a system composed of interconnected and interdependent components or elements that, as a whole, exhibit behaviors or properties that emerge from the interactions among those components. These systems are characterized by their nonlinearity, dynamic nature, and often have a large number of elements. Soon, we'll explore the suggested model by using various tools and ideas like special math operations (fractal-fractional), fuzzy math concepts, and random processes (stochastic concepts).

Acknowledgment

All authors are thankful to Prince Sultan University for APC and support through TAS research lab.

References

[1] X. Abdurahman, L. Zhang, Z. Teng, *Global dynamics of a discretized heroin epidemic model with time delay*, Abstr. Appl. Anal., **2014** (2014), 10 pages. 1

[2] R. P. Agarwal, A. M. A. El-Sayed, S. M. Salman, *Fractional-order Chua's system: discretization, bifurcation and chaos*, Adv. Differ. Equ., **2013** (2013), 13 pages.

[3] Z. Ahmad, F. Ali, A. M. Alqahtani, N. Khan, I. Khan, *Dynamics of cooperative reactions based on chemical kinetics with reaction speed: A comparative analysis with singular and nonsingular kernels*, Fractals, **30** (2022), 22 pages. 1

[4] Z. Ahmad, F. Ali, N. Khan, I. Khan, *Dynamics of fractal-fractional model of a new chaotic system of integrated circuit with Mittag-Leffler kernel*, Chaos Solitons Fractals, **153** (2021), 20 pages. 1

[5] Z. Ahmad, G. Bonanomi, D. di Serafino, F. Giannino, *Transmission dynamics and sensitivity analysis of pine wilt disease with asymptomatic carriers via fractal-fractional differential operator of Mittag-Leffler kernel*, Appl. Numer. Math., **185** (2023), 446–465. 1

[6] S. Ahmad, M. F. Yassen, M. M. Alam, S. Alkhati, F. Jarad, M. B. Riaz, *A numerical study of dengue internal transmission model with fractional piecewise derivative*, Results Phys., **39** (2022), 1–9. 1

[7] A. A. Alshareef, H. A. Batarfi, *Stability analysis of chain, mild and passive smoking model*, Am. J. Comput. Math., **10** (2020), 31–42. 1

[8] C. Castillo-Garsow, G. Jordan-Salivia, A. Rodriguez-Herrera, *Mathematical models for the dynamics of tobacco use, recovery and relapse*, In: Technical Report Series BU-1505-M, Cornell University, Ithaca, NY, USA, (1997). 1

[9] G. Huang, A. Liu, *A note on global stability for a heroin epidemic model with distributed delay*, Appl. Math. Lett., **26** (2013), 687–691. 1

[10] S. Hussain, Tunç, G. ur Rahman, H. Khan, E. Nadia, *Mathematical analysis of stochastic epidemic model of MERS-corona & application of ergodic theory*, Math. Comput. Simul., **207** (2023), 130–150. 1, 4.4

[11] M. M. M. Ihsanjaya, N. Susyanto, *Mathematical model of changes in smoking behavior which involves smokers who temporarily and permanently quit smoking*, AIP Conf. Proc., **2019** (2019), 1–9. 1

[12] H. Khan, S. Ahmed, J. Alzabut, A. T. Azar, *A generalized coupled system of fractional differential equations with application to finite time sliding mode control for Leukemia therapy*, Chaos Solitons Fractals, **174** (2023), 12 pages. 1

[13] N. Khan, F. Ali, Z. Ahmad, S. Murtaza, A. H. Ganie, I. Khan, S. M. Eldin, *A time fractional model of a Maxwell nanofluid through a channel flow with applications in grease*, Sci. Rep., **13** (2023), 15 pages. 1

[14] N. Khan, A. Ali, A. Ullah, Z. A. Khan, *Mathematical analysis of neurological disorder under fractional order derivative*, AIMS Math., **8** (2023), 18846–18865. 1

[15] H. Khan, J. Alzabut, A. Shah, Z. Y. He, S. Etemad, S. Rezapour, A. Zada, *On fractal-fractional waterborne disease model: A study on theoretical and numerical aspects of solutions via simulations*, Fractals, **31** (2023), 16 pages. 1

[16] M. A. Khan, S. Ullah, S. Kumar, *A robust study on 2019-nCOV outbreaks through non-singular derivative*, Eur. Phys. J. Plus., **136** (2021), 20 pages. 1

[17] S. Kumar, R. P. Chauhan, S. Momani, S. Hadid, *Numerical investigations on COVID-19 model through singular and non-singular fractional operators*, Numer. Methods Partial Differential Equations, **40** (2024), 27 pages. 1

[18] S. Kumar, R. Kumar, C. Cattani, B. Samet, *Chaotic behaviour of fractional predator-prey dynamical system*, Chaos Solitons Fractals, **135** (2020), 12 pages. 1

[19] S. Kumar, A. Kumar, B. Samet, H. Dutta, *A study on fractional host-parasitoid population dynamical model to describe insect species*, Numer. Methods Partial Differential Equations, **37** (2021), 1673–1692. 1

[20] X. Li, R. P. Agarwal, J. F. Gómez-Aguilar, Q. Badshahd, G. ur Rahman, *Threshold dynamics: formulation, stability & sensitivity analysis of co-abuse model of heroin and smoking*, Chaos Solitons Fractals, **161** (2022), 18 pages. 1, 4.2.1, 4.3, 5

[21] C. Li, F. Zeng, *The finite difference methods for fractional ordinary differential equations*, Numer. Funct. Anal. Optim., **34** (2013), 149–179. 1

[22] S. Liu, L. Zhang, X.-B. Zhang, A. Li, *Dynamics of a stochastic heroin epidemicmodel with bilinear incidence and varying population size*, Int. J. Biomath., **12** (2019). 1

[23] C. Lucas, J, Martin, *Smoking and drug interactions*, Aust. Prescr., **36** (2013), 102–104a. 1

[24] S. A. Matintu, *Smoking as epidemic: modeling and simulation study*, Am. J. Appl. Math., **5** (2017), 31–38. 1

[25] H. Mohammadi, S. Kumar, S. Rezapour, S. Etemad, *A theoretical study of the Caputo-Fabrizio fractional modeling for hearing loss due to mumps virus with optimal control*, Chaos Solitons Fractals, **144** (2021), 13 pages. 1

[26] S. Murtaza, P. Kumam, T. Sutthibutpong, P. Suttiarporn, T. Srisurat, Z. Ahmad, *Fractal-fractional analysis and numerical simulation for the heat transfer of ZnO + Al2O3 + TiO2/DW based ternary hybrid nanofluid*, ZAMM - J. Appl. Math. Mech./ZAMM Z. fur Angew. Math., **104** (2024). 1

[27] I. Podlubny, *Fractional differential equations*, Academic Press, San Diego, CA, (1999). 1

[28] A. M. Pulecio-Montoya, L. E. Lopez-Monteneqro, L. M. Benavides, *Analysis of a mathematical model of smoking*, Contemp. Eng. Sci., **12** (2019), 117–129. 1

[29] H. Qu, M. ur Rahman, S. Ahmad, M. B. Riaz, M. Ibrahim, T. Saeed, *Investigation of fractional order bacteria dependent disease with the effects of different contact rates*, Chaos Solitons Fractals, **159** (2022), 8 pages. 1

[30] S. G. Samko, A. A. Kilbas, O. I. Marichev, *Fractional integrals and derivatives*, Gordon and Breach Science Publishers, Yverdon, (1993). 1

[31] I. Ullah, A. Ali, S. Saifullah, *Analysis of time-fractional non-linear Kawahara Equations with power law kernel*, Chaos Solitons Fractals: X, **9** (2022) 1–8. 1
[32] G. ur Rahman, R. P. Agarwal, Q. Din, *Mathematical analysis of giving up smoking model via harmonic mean type incidence rate*, Appl. Math. Comput., **354** (2019), 128–148. 1
[33] P. Veeresha, D. G. Prakasha, H. M. Baskonus, *Solving smoking epidemic model of fractional order using a modified homotopy analysis transform method*, Math. Sci. (Springer), **13** (2019), 115–128. 1
[34] X. Wang, J. Yang, X. Li, *Dynamics of a Heroin epidemic model with very population*, Appl. Math. (Irvine), **2** (2011), 732–738. 1
[35] E. White, C. Comiskey, *Heroin epidemics, treatment and ODE modelling*, Math. Biosci., **208** (2007), 312–324. 1
[36] WHO, Tobacco, https://www.who.int/news-room/fact-sheets/detail/tobacco [Accessed 24 May 2019]. 1
[37] C. Xu, Z. Liu, P. Li, J. Yan, L. Yao, *Bifurcation mechanism for fractional-order three-triangle multi-delayed neural networks*, Neural Process. Lett., **55** (2023), 6125–6151. 1
[38] C. Xu, D. Mu, Z. Liu, Y. Pang, M. Liao, C. Aouiti, *New insight into bifurcation of fractional-order 4D neural networks incorporating two different time delays*, Commun. Nonlinear Sci. Numer. Simul., **118** (2023) 41 pages. 1
[39] C. Xu, W. Zhang, C. Aouiti, Z. Liu, L. Yao, *Bifurcation insight for a fractional-order stage-structured predator-prey system incorporating mixed time delays*, Math. Methods Appl. Sci., **46** (2023), 9103–9118. 1